The *Mycobacterium tuberculosis* Stress Response Factor SigH Is Required for Bacterial Burden as Well as Immunopathology in Primate Lungs

Smriti Mehra,[1] Nadia A. Golden,[1] Kerstan Stuckey,[1] Peter J. Didier,[2] Lara A. Doyle,[3] Kasi E. Russell-Lodrigue,[3] Chie Sugimoto,[4] Atsuhiko Hasegawa,[4] Satheesh K. Sivasubramani,[5] Chad J. Roy,[5] Xavier Alvarez,[2] Marcelo J. Kuroda,[4] James L. Blanchard,[3] Andrew A. Lackner,[2,6] and Deepak Kaushal[1,6]

[1]Division of Bacteriology and Parasitology, [2]Division of Comparative Pathology, [3]Division of Veterinary Medicine, [4]Division of Immunology, and [5]Division of Microbiology, Tulane National Primate Research Center, Covington, and [6]Department of Microbiology and Immunology, Tulane University Health Sciences Center, New Orleans, Louisiana

(See the editorial commentary by Kernodle, on pages 1186–8.)

Background. Sigma H (sigH) is a major *Mycobacterium tuberculosis* (*Mtb*) stress response factor. It is induced in response to heat, oxidative stress, cell wall damage, and hypoxia. Infection of macrophages with the Δ-sigH mutant generates more potent innate immune response than does infection with *Mtb*. The mutant is attenuated for pathology in mice.

Methods. We used a nonhuman primate (NHP) model of acute tuberculosis, to better understand the phenotype of the Δ-sigH mutant in vivo. NHPs were infected with high doses of *Mtb* or the mutant, and the progression of tuberculosis was analyzed in both groups using clinical, pathological, microbiological, and immunological parameters.

Results. Animals exposed to *Mtb* rapidly progressed to acute pulmonary tuberculosis as indicated by worsening clinical correlates, high lung bacterial burden, and granulomatous immunopathology. All the animals rapidly succumbed to tuberculosis. On the other hand, the NHPs exposed to the *Mtb*:Δ-sigH mutant did not exhibit acute tuberculosis, instead showing significantly blunted disease. These NHPs survived the entire duration of the study.

Conclusions. The *Mtb*:Δ-sigH mutant is completely attenuated for bacterial burden as well as immunopathology in NHPs. SigH and its regulon are required for complete virulence in primates. Further studies are needed to identify the molecular mechanism of this attenuation.

Tuberculosis is responsible for the deaths of >1.7 million people annually [1]. This situation is exacerbated by the emergence of drug-resistant *Mycobacterium tuberculosis* (*Mtb*) [2, 3], AIDS coinfection [4], and the failure of the BCG vaccine [5]. Development of efficacious treatments and vaccines against tuberculosis will require better understanding of the pathogenesis of *Mtb*.

Alternative sigma (σ) factors allow bacteria to respond to changes in the extracellular environment by modulating the expression of specific sets of genes [6]. The temporal expression of specific regulons controlled by the induction of ≥1 of the 10 alternate σ factors [7] encoded by its genome may allow *Mtb* to survive in diverse environments encountered by it in vivo. Sigma H (sigH) is an alternate σ factor induced by various stress conditions, phagocytosis, cell wall damage, enduring hypoxia, and reaeration and possibly plays a role in reactivation [8–19]. The Δ-sigH mutant fails to induce granulomatous pathology in spite of bacterial replication in mice [8]. Infection of nonhuman primate (NHP) bone-marrow macrophages with *Mtb*:Δ-sigH results in a significantly enhanced monocyte chemotaxis and

Received 9 June 2011; accepted 16 September 2011; electronically published 7 March 2012.

Presented in part: Keystone Symposia on Molecular and Cellular Biology: Mycobacteria: Physiology, Metabolism, and Pathenogenesis—Back to Basics, Vancouver, British Columbia, Canada, 14–19 January 2011.

Correspondence: Deepak Kaushal, PhD, Division of Bacteriology and Parasitology, Tulane National Primate Research Center, 18703 Three Rivers Rd, Covington, LA 70433 (dkaushal@tulane.edu).

The Journal of Infectious Diseases 2012;205:1203–13

DOI: 10.1093/infdis/jis102

apoptosis relative to cells infected with *Mtb* [20]. Thus, sigH appears to code for functions crucial for modulating immune response.

Due to their physiological and immunological similarity to humans, NHPs are excellent experimental models of tuberculosis [21, 22]. Two key NHP models of tuberculosis exist. One model is based on infected cynomolgus macaques with virulent *Mtb* via the intratracheal route [22]. The other model is based on infection of rhesus macaques with virulent *Mtb* via the aerosol route mimicking the natural method of exposure [23–25]. By modulating the number of infectious aerosols presented, it is possible to model either acute [23, 24] or latent [25] tuberculosis in these NHPs. The number of presented aerosols is standardized by plethsymography immediately prior to infection. The acute model is used to understand bacterial pathogenesis, whereas the latent model is used to study the various mediators of latency, reactivation, and tuberculosis/AIDS coinfection [25]. We employed the acute model to address whether sigH is important for growth and replication of *Mtb* as well as immunopathology in primates.

MATERIALS AND METHODS

Animals and Infection

Animals were cared for according to the National Institutes of Health (NIH) Guide for the Care and Use of Laboratory Animals and Institutional Animal Care and Use Committee guidelines. Aerosol infection of 13 Indian-origin rhesus macaques (Table 1) was performed as described elsewhere [23, 25]. Seven animals were exposed to a high-dose (approximately 5000 colony-forming units [CFUs]) of *Mtb* CDC1551. Six NHPs were similarly exposed to the *Mtb*:Δ-sigH mutant. Blood, bronchoalveolar lavage (BAL), and peripheral lymph node (LN) samples were collected periodically. Clinical assessment of disease, C-reactive protein (CRP) assay, chest radiography (CXR), tuberculin skin test (TST), necropsy, and histopathology procedures, including the analysis of percentage of the lung area involved in tuberculosis-like pathology, have been described in NHPs [23, 25, 26].

Bacterial Burden

Viable CFUs were compared in periodic BAL fluid and LN homogenates as well as random lung section homogenates at necropsy as described elsewhere [23, 25], to measure the burden of viable tubercle bacilli. For confocal microscopy based detection of the bacilli in the lung lesions, a polyclonal anti-*Mtb* antibody raised in rabbit (Abcam ab905) was used as described elsewhere [23–26].

Comparison of Granulomatous Gene-Expression Upon Infection With *Mtb* and *Mtb*:Δ-sigH

DNA microarray experiments were performed as described elsewhere [24]. Transcripts isolated from 3 randomly chosen NHPs from each group were profiled, relative to normal rhesus lung tissue.

Immunohistochemistry and Confocal Microscopy

$CD3^+$, $FoxP3^+$, and $CD25^+$ cells in tissues were counted by immunohistochemistry as described elsewhere [27]. The following

Table 1. Animals Infected With *Mycobacterium tuberculosis* (*Mtb*) or the *Mtb*:Δ-sigH Mutant and Their Tuberculin Skin Test Results

ID	Infecting Agent	Age at Infection (Years)	Weight at Infection (kg)	Time to Death (Days)	Time to Experiment Death (Days)	TST (Preinfection)	TST (Week 3)	TST (Week 9)
CG58	*Mtb*	7.50	11.40	75		NNN	PPP	P[a]
DJ57	*Mtb*	5.80	12.65	75		NNN	PPP	P[a]
HB38	*Mtb*	3.20	5.00	71		NNN	PPP	NC
HB43	*Mtb*	3.20	5.30	56		NNN	NPP	NC
GN05	*Mtb*	4.02	6.30	57		NNN	PPP	NC
GK47	*Mtb*	4.10	6.70	49		NNN	NPP	NC
GM97	*Mtb*	4.02	5.70	79		NNN	PPP	PPP
CC41	*Mtb*:Δ-sigH	7.75	14.20		76	NNN	PPP	P[a]
DM75	*Mtb*:Δ-sigH	5.80	12.55		76	NNN	PPP	P[a]
EE62	*Mtb*:Δ-sigH	8.13	14.00		70	NNN	NPP	PPP
DE35	*Mtb*:Δ-sigH	9.17	13.30		70	NNN	NPP	PPP
GM51	*Mtb*:Δ-sigH	4.03	5.50		71	NNN	PPP	PPP
HC50	*Mtb*:Δ-sigH	3.17	5.60		71	NNN	NNN	PPP

Shown are the unique Tulane National Primate Resource Center–assigned IDs, age and weight at infection, and time to death or experimental euthanasia following infection. Results from eyelid TST are also described for 3 different time points: preinfection and weeks 4 and 8 postinfection [33]. Results were measured at 24, 48, and 72 hours postadministration.

Abbreviations: N, negative; NC, not conducted; NNN, a negative TST was recorded at each of the 3 time points (24, 48, and 72 hours); NPP, a positive TST was recorded at the 48- and 72-hour time points only; P, positive; PPP, a positive TST at each of the 3 time points; TST, tuberculin skin test.

[a] PRIMAGAM, an interferon γ release assay, was substituted for TST [33].

antibodies were used: anti-CD3 (Dako-A0452, rabbit, 1:50); antiFoxP3 (Vector Labs- VP-C340, mouse, 1:50) and anti-CD25 (eBioscience-14-4776-82, rat, 1:50). Multilabel confocal immunofluorescence was performed using previously described protocols [23–26] that used the following antibodies: interferon γ (IFN-γ) (1:10, mouse, BD Biosciences 551221); CD3 (1:10; mouse, Dako M7254), and FoxP3 (1:500; rabbit, Abcam ab10901).

Recruitment of Monocytes Derived From Bone Marrow Upon Infection

In vivo bromodeoxyuridine (BrdU) pulse-labeling and flow-cytometric analysis were performed as described elsewhere [28].

RESULTS

Comparison of Clinical Correlates of Infection in NHPs Infected With *Mtb*:Δ-sigH, Relative to Those Infected With *Mtb*

All 13 NHPs were negative for simian immunodeficiency virus (SIV), simian T-lymphotropic virus (STLV), simian retrovirus (SRV), and hepatitis B virus. All NHPs converted to a positive TST within 3–5 weeks postinfection, indicating successful infection (Table 1). TST was read at 24, 48, and 72 hours postadministration. Positive TST result was obtained for all 13 NHPs at 72 hours and for most NHPs at 48 and 24 hours. The animals infected with *Mtb* began exhibiting clinical features associated with acute tuberculosis within 3–4 weeks postinfection. In total, 6 of 7 NHPs in this group had elevated temperatures of >2°F higher than average preinfection temperatures at the week 3 postinfection time point, whereas none of the 6 NHPs exposed to *Mtb*:Δ-sigH experienced a significant increase in body temperature at any time during the study (Figure 1*A*).

The *Mtb*-infected NHPs exhibited significant weight loss over the study period, losing 5%–25% of their body weight over the duration of the study (Figure 1*B*). In fact, by week 7 postinfection, the NHPs in this group had lost an average of approximately 12% in body weight. In contrast, the NHPs in the mutant-infected group gained an average of 7% body weight during the study (Figure 1*B*).

NHPs infected with *Mtb* are known to exhibit increased serum levels of acute-phase proteins such as CRP. We therefore studied serum levels of CRP to measure systemic inflammation, over the course of infection [23, 25–27]. The serum CRP levels spiked in each of the 7 *Mtb*-infected NHPs between 3 and 6 weeks postinfection (Figure 1*C*) and were significantly elevated relative to preinfection baseline for each of the 7 NHPs (Figure 1*C*). At week 3 postinfection, the CRP values for the NHPs in this group ranged from 3.26 to 44.75 mg/L, as compared with preinfection values ranging from 0.0 to 0.4 mg/L. The mutant-infected NHPs did not exhibit elevated CRP values. The maximal CRP value for the mutant-infected NHPs throughout the study was 2.5 mg/L. Only 2 animals in this group exhibited higher than baseline CRP values at any time point but with significantly lower magnitude. The differences between the 2 groups were significant from week 3 postinfection onward (Figure 1*C*).

CXRs from these NHPs were assigned a subjective score on a scale of 0–3, using the following scoring criterion: no involvement, 0; minimal disease, 1; moderate disease, 2; and severe/miliary disease, 3 [23, 25]. All NHPs infected with *Mtb* exhibited gradually increasing CXR scores that were significantly higher than baseline scores at weeks 3 and 7 postinfection. The mutant infected animals indicated significantly lower CXR scores (Figure 1*D*). These results corroborate the lack of progression of tuberculosis in NHPs infected with *Mtb*:Δ-sigH, relative to NHPs infected with *Mtb*, in this high-dose, acute disease model.

Survival Differences Between the 2 Groups of NHPs

Differences in the progression of tuberculosis in NHPs infected with *Mtb* vs *Mtb*:Δ-sigH were apparent in the survival of the 2 groups. All 7 NHPs infected with *Mtb* succumbed to acute, pulmonary tuberculosis within 13 weeks postinfection. The median time to death for this group was 65 days (Figure 1*E*). None of the animals infected with the mutant died during this period due to disease. These NHPs were experimentally killed. The survival proportions between the 2 groups were statistically significant (Figure 1*E*).

Bacterial Burden in NHPs Infected With *Mtb* and *Mtb*:Δ-sigH

We analyzed bacterial burden in BAL temporally at 3, 5, 9, and 11 week postinfection. A gradual increase in the number of viable *Mtb* CFUs was observed. In NHPs exposed to *Mtb*, viable CFU load was detected beginning week 5 postinfection, peaking at week 9 postinfection (average, $\sim 2 \times 10^3$ CFUs). No viable CFUs could be detected in the BAL fluid obtained from mutant-infected NHPs 5 week postinfection. Significantly low numbers of CFUs were recovered in the BALs of some NHPs in this group ($1–2 \times 10^2$ CFU) relative to the *Mtb* group at weeks 9 and 11 (Figure 2*A*).

Similarly, significantly high bacillary load was observed in the LNs of *Mtb*-infected NHPs, relative to mutant-infected NHPs. A higher load was observed for both groups at week 9 postinfection, relative to week 3 postinfection. The levels of *Mtb*:Δ-sigH in LNs were significantly lower relative to *Mtb* throughout the study (Figure 2*B*).

Finally, we assessed the *Mtb* load in lungs at the time of necropsy (Figure 2*C*). Average lung CFU values in *Mtb*-infected NHPs ranged from 7×10^3 to 8×10^4 CFUs/g. In contrast, the average lung CFUs in the mutant-infected NHPs were significantly lower, ranging from 0 to 3.3×10^2 CFUs/g (Figure 2*C*). The *Mtb*:Δ-sigH mutant exhibits a remarkably reduced bacterial burden in tissues compared with *Mtb*, in the NHP model.

The CFU results from BAL and lung were corroborated by immunofluorescence–based detection of bacilli in the lungs

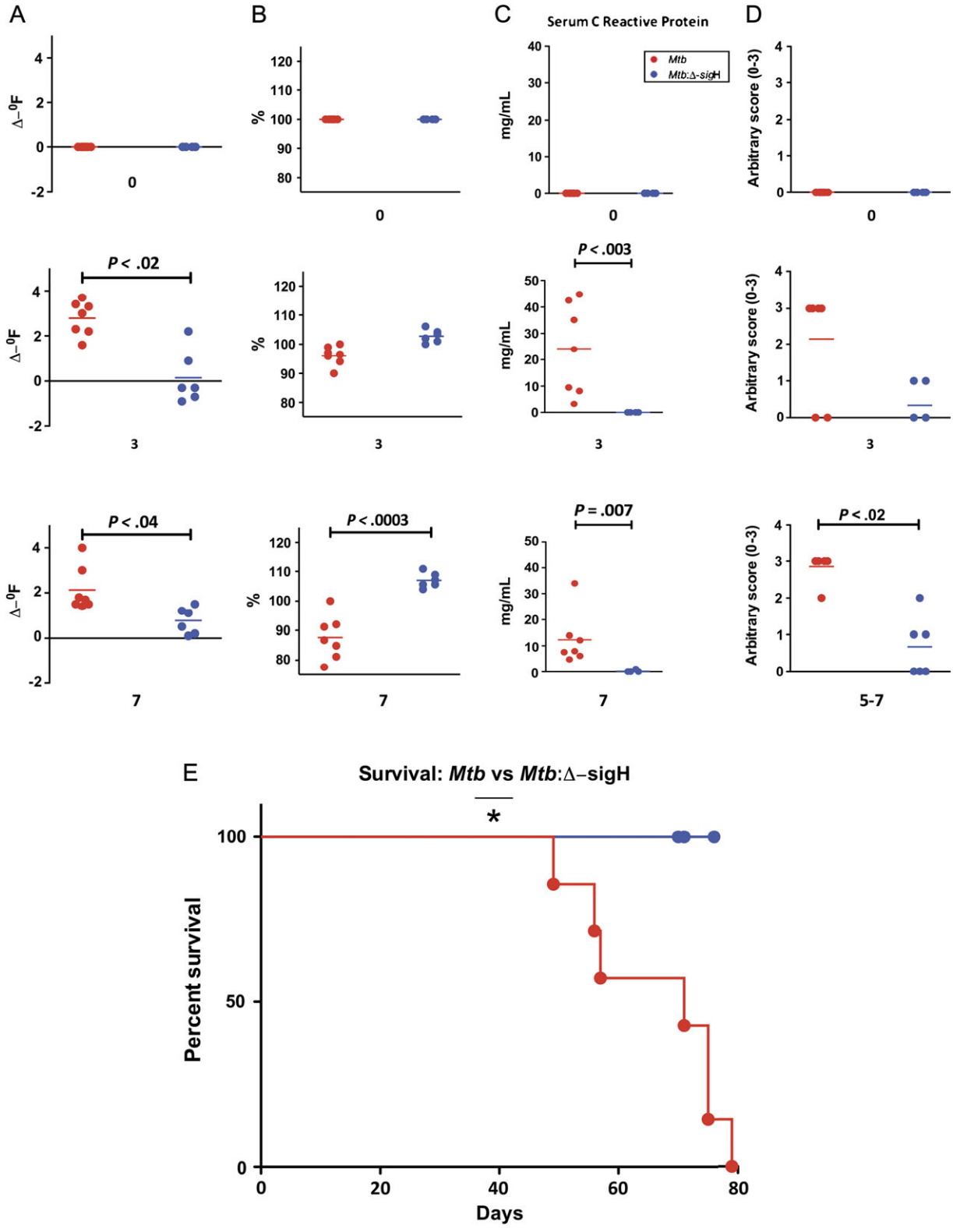

Figure 1. Clinical data from nonhuman primates (NHPs) infected with *Mycobacterium tuberculosis* (*Mtb*) as well as the *Mtb*:Δ-sigH mutant. *A*, Changes in body temperature, expressed in Δ-°F. *B*, Changes in body weight, expressed as percentage of total weight at the time of *Mtb* infection. *C*, Changes in serum C-reactive protein (CRP) levels. *D*, Changes in arbitrary chest radiographic (CXR) scores. *E*, Survival proportions. Data are shown for week 0 (preinfection) as well as weeks 3 and 7 postinfection for *A*, *B*, *C*, and *D*. The x-axis values represent week postinfection. Red circles denote NHPs infected with *Mtb,* whereas blue circles denote NHPs infected with the *Mtb*:Δ-sigH mutant. Significant differences are shown wherever detected.

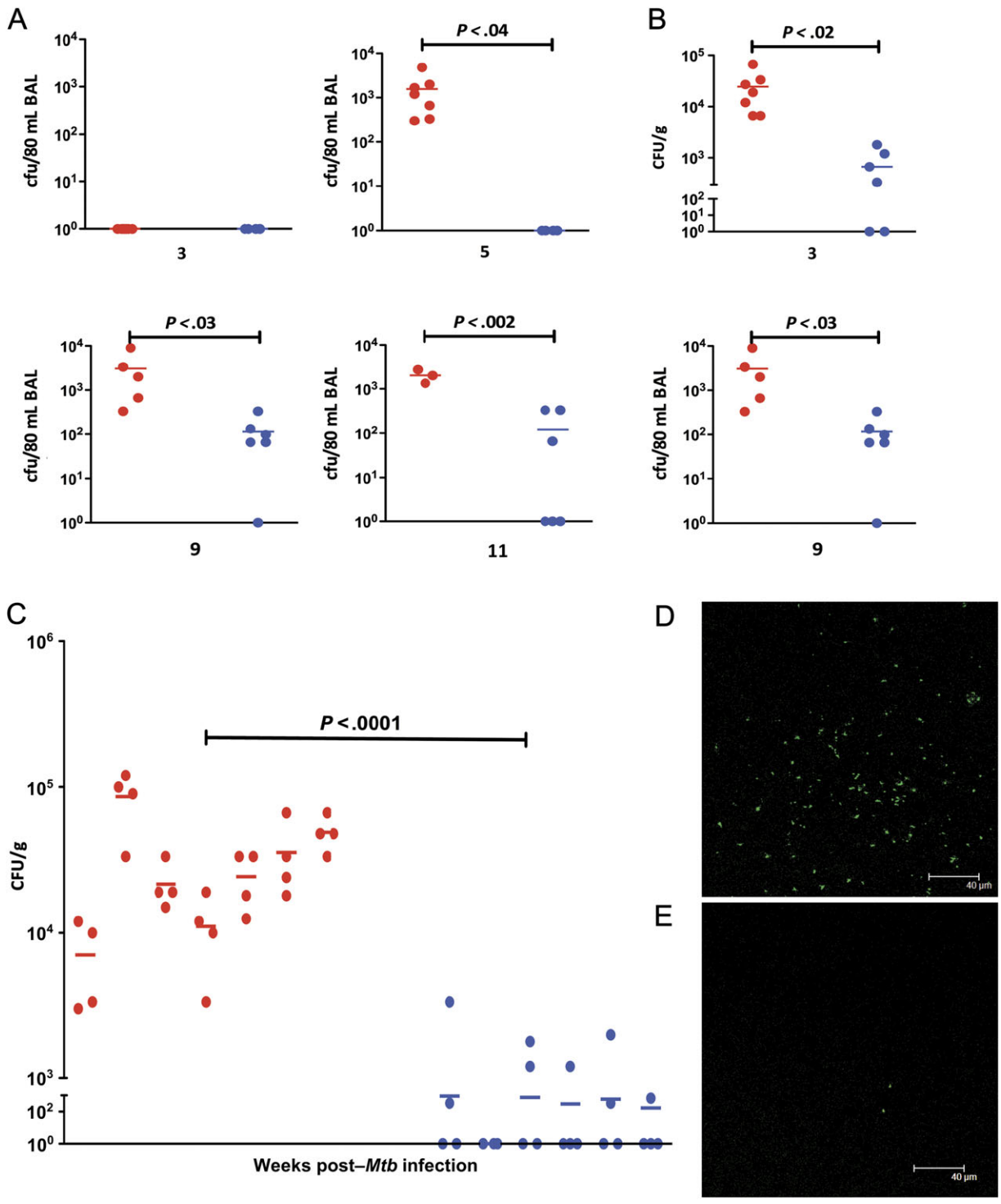

Figure 2. Bacterial burden in the 2 groups of nonhuman primates (NHPs). Temporal *Mycobacterium tuberculosis* (*Mtb*) colony-forming units (CFUs) are shown per 80 mL bronchoalveolar lavage (BAL) samples obtained from both groups of NHPs at weeks 3, 5, and 9 postinfection. *A*, Temporal *Mtb* CFUs are shown per gram of bronchial lymph node tissue obtained from both groups of NHPs at weeks 3 and 7 postinfection (*B*). *Mtb* colony-forming units (CFUs) are also shown per gram of lung tissue obtained at necropsy from both groups of NHPs (*C*). Each lung was randomly sectioned at necropsy and 10 sections from each of the 2 lungs were pooled into 2 groups (right lung 1, right lung 2; left lung 1, left lung 2). Results are shown for all 4 of these lung samples for each of the 13 NHPs. The *x*-axis values represent the week postinfection. Red circles denote NHPs infected with *Mtb,* and blue circles denote NHPs infected with the *Mtb*:Δ-sigH mutant. Confocal microscopy shows the extent of bacterial presence in the lungs of a representative NHP infected with *Mtb* (*D*) relative to a representative NHP infected with *Mtb*:Δ-sigH (*E*).

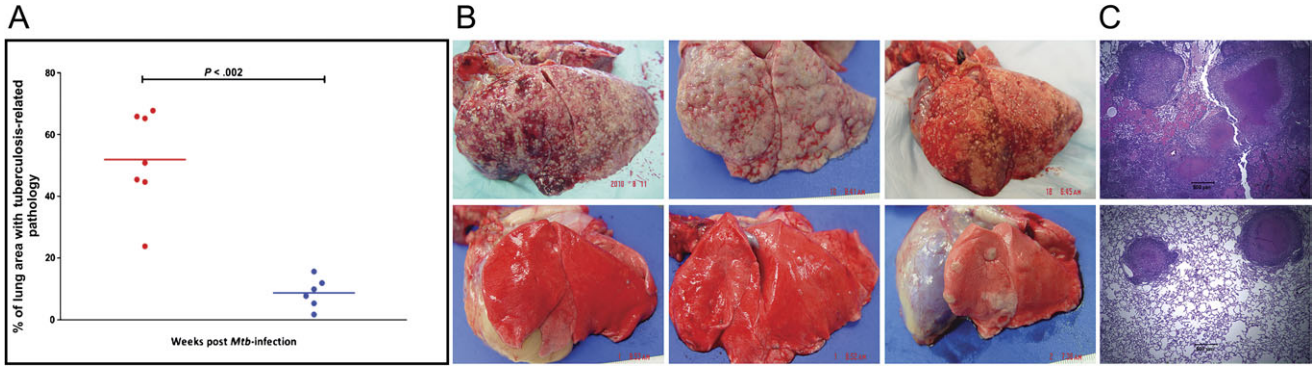

Figure 3. Postnecropsy pathology data from the 2 groups of nonhuman primates (NHPs). The percentage of lung area with tuberculosis-related pathology was estimated in both groups of NHPs (*A*) using methods described elsewhere [23, 25]. The *x*-axis values represent week postinfection. Red circles denote NHPs infected with *Mycobacterium tuberculosis* (*Mtb*), whereas blue circles denote NHPs infected with the *Mtb*:Δ-sigH mutant. Lines correspond to mean values. The differences between 2 groups were statistically significant. Gross pathology is shown for 3 representative NHPs each, infected with *Mtb* (*top panel*) and *Mtb*:Δ-sigH (*bottom panel*) (*B*). Histopathologic analysis of hematoxylin and eosin–stained lung samples from 1 representative NHP each, infected with *Mtb* (*top panel*) and *Mtb*:Δ-sigH (*bottom panel*) (*C*).

of *Mtb*- (Figure 2*D*) and mutant-infected NHPs (Figure 2*E*). Significantly higher levels of bacterial infection could be observed in the lungs of NHPs infected with *Mtb* (Figure 2*D*), whereas lungs of NHPs infected with the mutant were largely devoid of any bacilli (Figure 2*E*).

Lung Pathology in NHPs Infected With *Mtb*:Δ-sigH, Relative to Those Infected With *Mtb*

The NHPs infected with *Mtb* exhibited extensive pulmonary granulomatous immunopathology. The observed disease pathology was similar to an earlier study in which NHPs were exposed to a high dose of *Mtb* transposon mutants [23]. The extent of diseased tissue involved in tuberculous lesions (necrosis, granulomas, edema, etc) was calculated as a percentage of the total area (Figure 3). The average percentage of involvement in the lungs of *Mtb* and *Mtb*:Δ-sigH infected NHPs were 56.6% and 8.6%, respectively. Significant differences were apparent in lung lesions of the 2 groups (Figure 3*A*). Although the lungs of NHPs infected with high-dose *Mtb* exhibited multifocal and confluent graulomas (Figure 3*B*), the animals infected with the mutant exhibited relatively few and widely scattered lesions (Figure 3*B*). Histopathologic analysis using hematoxylin and eosin–stained lung tissues confirmed that the lesions observed in the NHPs infected with both *Mtb* and *Mtb*:Δ-sigH exhibited classical tuberculoid pattern with central necrosis and a peripheral infiltrate consisting of histiocytes, lymphocytes, and multinucleated giant cells (Figure 3*C*). NHPs infected with *Mtb* also exhibited acute inflammation with hemorrhage and neutrophilic infiltration suggesting concurrent chronic and rapid progression. Therefore, the infection with a high dose of *Mtb*:Δ-sigH produced a significantly and severely blunted tuberculosis disease.

Granulomatous Immune Response to Infection of NHPs With *Mtb*:Δ-sigH, Relative to *Mtb*

Using global transcriptomics, lung tubercular lesions from the 2 groups of NHPs were used to study changes in the pattern of immune response to infection [24]. Because we have already reported the transcriptome of primate lesions in response to *Mtb* infection at both the acute and the chronic stages [24], here we focused on genes that exhibit maximal significance in the magnitude of gene expression between the 2 groups, using multiple-hypothesis corrected *P* value (Figure 4*A*).

The expression of MMP9 (150-fold), CCL5 (28-fold), LTA (10-fold), and FOSB (4-fold) genes was induced to significantly higher levels in the lesions of *Mtb*-infected NHPs but remained at normal levels in lesions from the mutant-infected NHPs (Figure 4*A*). On the other hand, the expression of SOCS3 (8-fold), FOXJ1 (6-fold), BAX (5-fold), and CCL14 (3-fold) was induced to significantly higher levels in the lesions of mutant-infected NHPs, relative to *Mtb*-infected NHPs.

Because the expression of several proinflammatory genes was induced to higher levels in *Mtb* lesions, we studied the expression of the prototypical proinflammatory molecule, IFN-γ, by immunofluorescence. Lesions derived from *Mtb*-infected NHPs exhibited significantly high IFN-γ levels (Figure 4*B*), relative to lesions from mutant-infected NHPs (Figure 4*C*). We also studied the expression of the regulatory T cell (Treg) marker FoxP3 on T cells in these lesions by immunohistochemistry (Figure 5*A*–*C*) and immunofluorescence (Figure 5*D* and 5*E*). The total number of ($CD3^+$) T cells was significantly higher in the mutant lesions, relative to *Mtb* lesions (Figure 5*A* and 5*E*). This result is consistent with the fact that animals in the *Mtb* group exhibited acute pathology. However, the percentage of T cells that also exhibited FoxP3 expression was slightly higher in the mutant group,

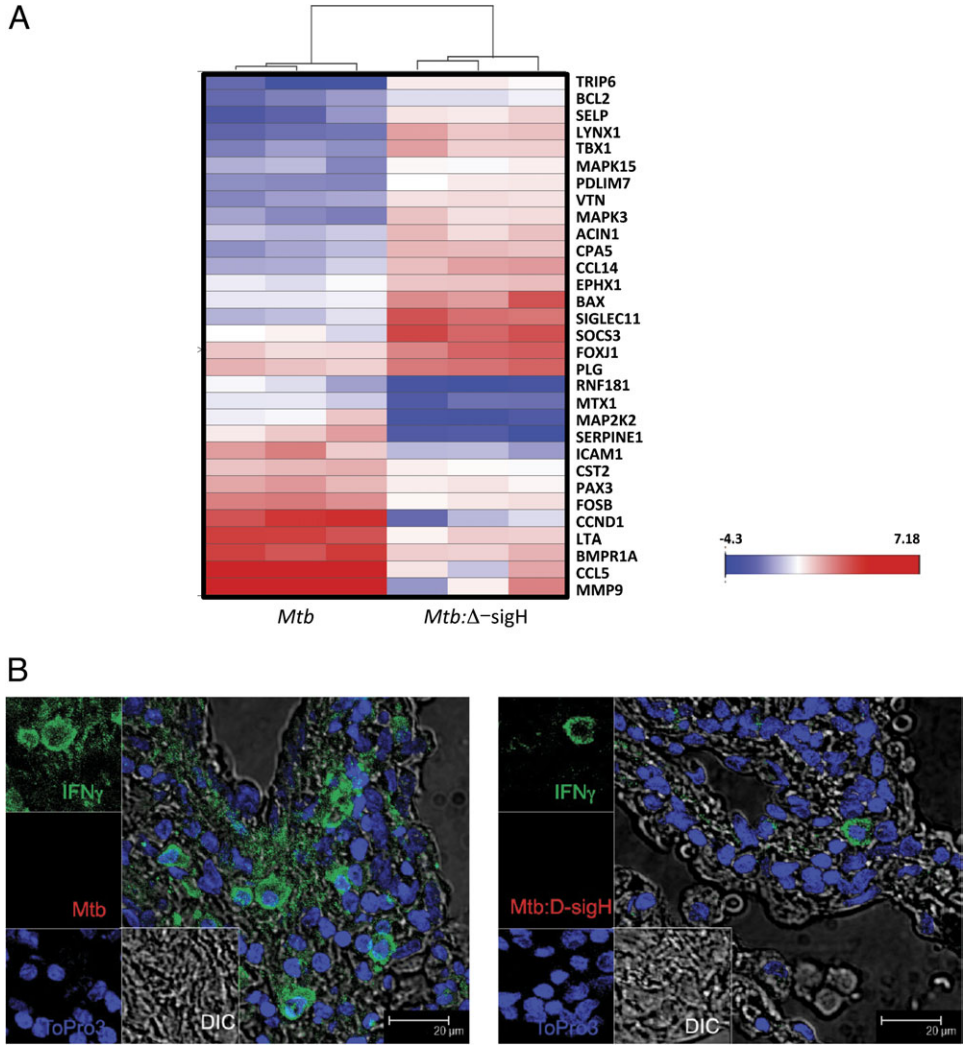

Figure 4. Immune response analysis using microarrays and confocal microscopy. Triplicate RNA samples derived from tuberculosis lesions of 3 nonhuman primates (NHPs) of each group were profiled on Agilent Rhesus Macaque 4 × 44 microarrays. The derived expression changes were sorted based on significance. Data are shown as heat-map clusters for genes with highly significantly differential expression in NHPs infected with *Mycobacterium tuberculosis* (*Mtb*) or the *Mtb*:Δ-sigH relative to the other group (*A*). The color schematics for the heat map are as follows: blue, lower expression relative to normal lung; white, comparable expression relative to normal lung; red, higher expression relative to normal lung. The intensity of red and blue color corresponds to the extent of induction or repression and is shown as a color bar (*A*). Multilabel confocal microscopy shows differential expression of the foremost anti-*Mtb* Th1 type proinflammatory cytokine interferon γ (IFN-γ) in the lung lesion of an NHP infected with *Mtb* (*B*) and *Mtb*:Δ-sigH (*C*). Eukaryotic cells were detected using a nuclear stain (TO-PRO3) (*blue signal*), and *Mtb* was detected using an *Mtb*-specific antibody (*red signal*), both as described elsewhere [23–26]. IFN-γ was detected using a specific antibody (*green signal*) as described in the "Materials and Methods" section.

although this difference was not significant (Figure 5*B* and 5*F*). The mutant-derived lesions also showed slightly higher number of T cells positive for CD25, an activation marker typically expressed on Tregs, but this difference was also not significant (Figure 5*C*).

Recruitment of Monocytes Derived From Bone Marrow During Infection With *Mtb* and *Mtb*:Δ-sigH

We compared the dynamic recruitment of monocytes in response to infection with *Mtb*, relative to infection with the mutant, in the 2 groups of NHPs at different stages of infection by in vivo BrdU labeling and flow cytometry. BrdU was injected 24 hours prior to bleeds [28]. Four animals in each group were used for these assays. No differences in BrdU incorporation was observed in the 2 groups pre-infection (Figure 6*A*). However, at 4–5 weeks postinfection, the level of $BrdU^+$ monocytes was significantly higher in the blood of *Mtb*-infected NHPs, relative to the mutant-infected group (Figure 6*B*). Only 2 NHPs in the mutant group exhibited an increase in the incorporation of BrdU in $CD14^+$ over

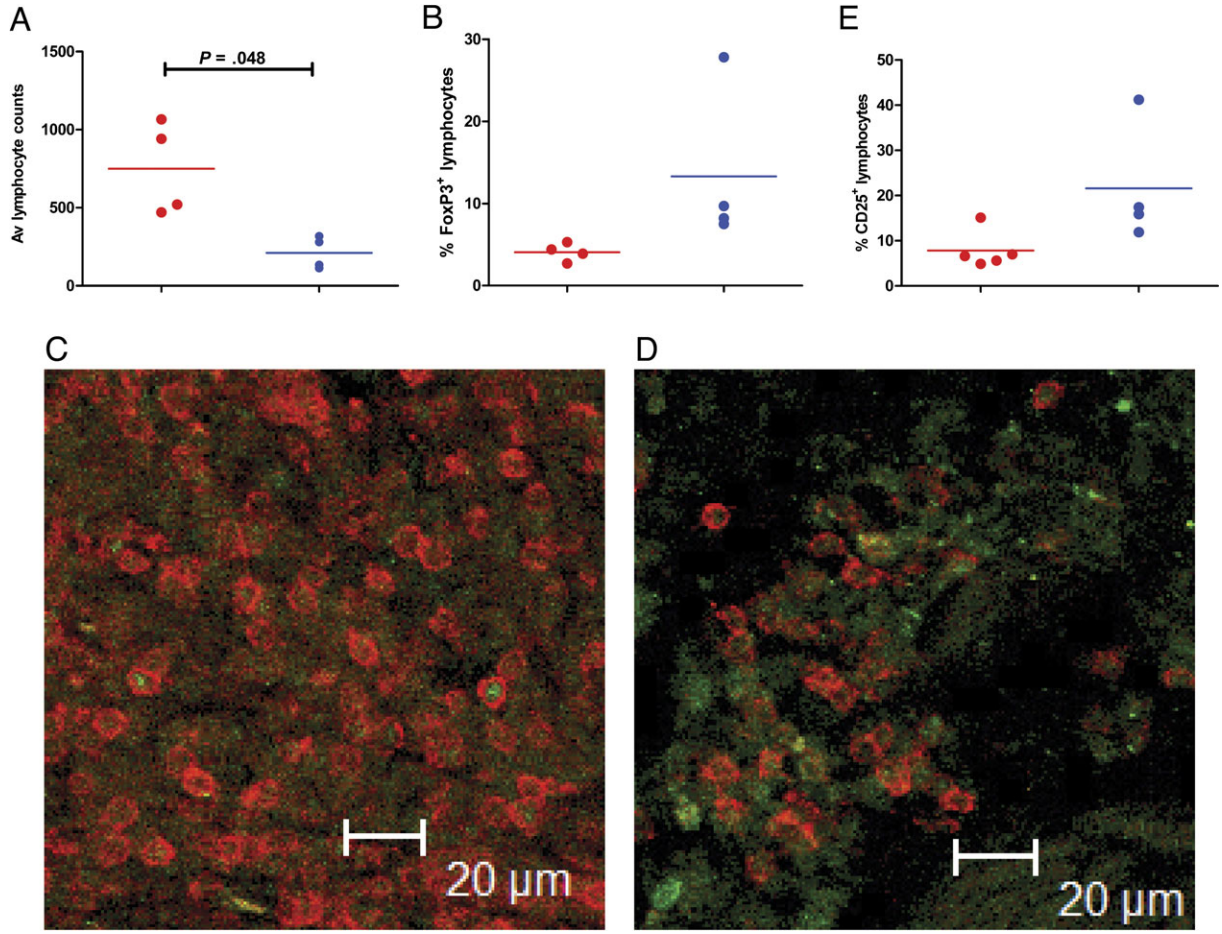

Figure 5. Identification of regulatory T cells (Tregs) in the tubercle lesions of the 2 groups of nonhuman primates (NHPs). Immunohistochemisty (*A–C*) and immunofluorescence were performed to identify total $CD3^+$ T cells (*A, D*), $CD3^+$ $FoxP3^+$Tregs (*B, E*), and $CD3^+CD25^+$ activated Tregs (*E*). For immunohistochemical determination of total numbers, 6 fields per slide were counted for 4 NHPs in each group at ×20 magnification using a Leica DMLB scope and a SPOT Insight Color 3.2.0 camera. Images were taken with SPOT 3.4.5 software and counted using Image Pro-Plus 4.5.0.19.

baseline values, but the magnitude of this increase was substantially lower than that observed in all 4 NHPs from the *Mtb* group. These differences were highly significant.

DISCUSSION

The work of several laboratories has established that sigH is a major stress response factor of *Mtb* [8–10] that is either directly or indirectly involved in coordinating the pathogen's response to a wide variety of stress conditions [8–19]. The *Mtb*:Δ-sigH mutant is attenuated for pathology but not *Mtb* replication in mice [8], and more susceptible to a variety of stress conditions [9, 10, 15]. A significantly higher number of *Mtb* mutants are attenuated in NHPs, compared with murine lungs [23]. We therefore hypothesized that the *Mtb*:Δ-sigH mutant may be attenuated for bacterial growth in the NHP model.

The *Mtb*:Δ-sigH mutant elicits a more robust immune response upon infecting host macrophages, relative to infection with *Mtb* [20]. This greater immune response is characterized by significantly higher levels of β-chemokine secretion and chemotaxis of naive monocytes, and a higher degree of apoptosis [20]. Similar results have been reported for SigE, a related alternate σ factor [29]. It is therefore conceivable that SigH and SigE induce the expression of molecule(s) that interact with and modulate chemotaxis and apoptosis by host macrophages. Conceivably, this would aid *Mtb* in its persistence and dissemination of the initial infection, because chemotaxis is necessary for activated immune cells to arrive at the initial site of infection [30], and apoptosis is a key mechanism for the innate clearance of *Mtb* [31]. Therefore, we also hypothesize that infection of NHPs with the *Mtb*:Δ-sigH mutant will elicit a much stronger immune response than with *Mtb* alone. This scenario is consistent with the hypothesis that increased SigH and other antioxidative mechanisms are responsible for reduced immunogenicity of the BCG vaccine strains [32, 33]. We have devised experiments to test whether

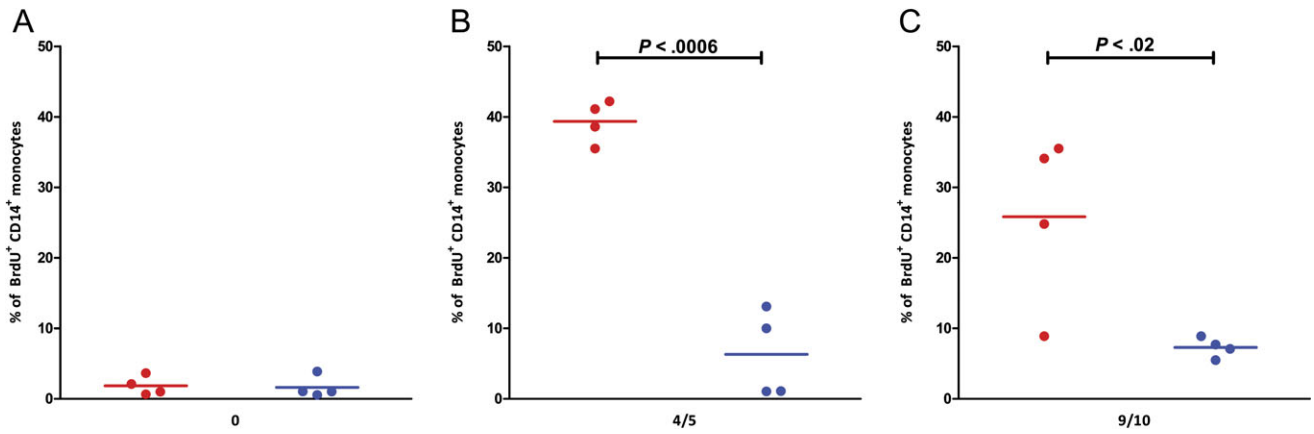

Figure 6. In vivo bromodeoxyuridine (BrdU) labeling and flow cytometry. Four animals from each group were injected with BrdU (10 mg/kg body weight) as described elsewhere [28], prior to infection (*A*) and 4–5 weeks postinfection (*B*). Blood was collected 24 hours after BrdU inoculation. The percentages of BrdU-positive cells in $CD14^+$ monocytes were analyzed by flow cytometry as described elsewhere [28].

the *Mtb*:Δ-sigH mutant is attenuated for both bacterial infection in the NHP model.

Clinical, microbiological, and pathological assays show that the *Mtb*:Δ-sigH mutant is attenuated for both bacterial burden and immunopathology. Although NHPs infected with *Mtb* developed acute tuberculosis and died within weeks, the NHPs infected with the mutant remained completely devoid of disease. Therefore, the *Mtb* sigH regulon is required for full virulence in primates. Specific mechanisms behind this significant attenuation are presently unclear. It is possible that the rate of intrinsic replication of the mutant is reduced in vivo. On the basis of the known functions of SigH, however, and the fact that *Mtb*:Δ-sigH exhibits no effect of the mutation during in vitro growth, this is not the likeliest of possibilities. Alternatively, it is possible that the mutant is relatively more susceptible to host innate immunity. SigH is strongly induced in response to redox stress and phagocytosis and may play a role in countering oxidative burst [8–10]. It is therefore plausible that the reduced burden of the mutant reflects greater susceptibility to phagocyte oxidative burst. Another possibility is that the *Mtb*:Δ-sigH strain is incapable of immunomodulating adverse host responses. Our in vitro results that phagocytes infected with *Mtb*:Δ-sigH exhibit higher levels of chemotaxis and apoptosis, raise the possibility that antigen(s) regulated by SigH negatively modulate innate phagocytic immune responses and the loss of SigH in the mutant strain unmasks this effect. The current experimental design is insufficient to differentiate between these possibilities. The use of technologies such as unstable plasmids with finite rate of exclusion will allow us to differentiate between replication rate and bacterial burden in vivo [34]. We are now studying the temporal immune response to infection with these strains to better understand the mechanism of attenuation. We are also trying to identify the bacterial factors involved in potentially modulating phagocyte responses.

The induction of MMP9, which promotes granulomatous pathology [35, 36], CCL5, involved in chemotaxis, LTA, involved in the control of chronic *Mtb* infection [37], and FOSB, known to be induced in a tumor necrosis factor–dependent manner [38], is consistent with our current understanding. However, proteins that are relatively more abundant in mutant lesions may be more important in understanding the mechanism of attenuation. The proapoptotic BCL2 family member BAX is involved in cell death induced by cytotoxic T cells [39]. Its increased levels in the mutant lesions may be due to increased cytotoxic lymphocyte activity in the lungs of macaques infected with the mutant. Interestingly, modifications that reduce the production of *Mtb* antioxidants (eg, sigH or sodA) enhance CD8 T-cell responses [32, 40]. In the future, we will design experiments to specifically address this hypothesis.

Alternatively, the attenuation with *Mtb*:Δ-sigH may result from the unmasking of Tregs that reduce overexuberant proinflammatory response. Oxidants are reported to significantly reduce tissue inflammation [41]. We observed that the expression of SOCS3, which targets STATs [42], and FOXJ1, which modulates inflammatory reactions by interfering with the NFκβ pathway [43], was significantly higher in mutant lesions. Recent reports suggest that in an NHP model of tuberculosis, instead of acute disease, the frequency of Tregs was correlated directly to the ability to control infection in a latent state [44]. Because our expression analysis supported the hypothesis that the attenuation of *Mtb*:Δ-sigH may be at least in part from reduced inflammation due to Treg activity, we performed experiments to measure Tregs in the lung lesions of the 2 groups. Not surprisingly, total $CD3^+$ cells were higher in *Mtb* lesions. However, slightly higher

Treg numbers were seen in the mutant lesions (Figure 5). Moreover, the activation status of Tregs (measured by CD25 staining) was also slightly higher in the mutant group. Interestingly, FoxP3 staining was also observed in the mutant group in $CD3^-$ cells (Figure 5*E*). Although we do not know the identity of these cells at the present time, $FoxP3^+$ macrophages have been recently reported to play roles in modulating inflammation [45]. These results suggest that active suppression of inflammation may be of benefit to the host.

BrdU is a reliable marker for dividing cells. Because blood monocytes are unable to proliferate in circulation, they do not incorporate BrdU. Thus, BrdU-labeled monocytes can be considered to have recently migrated from the bone marrow [28]. In vivo BrdU labeling indicates massive destruction of lung macrophages during active tuberculosis. These results are corroborated by the 150-fold induction of MMP9 levels in these lungs.

When the *Mtb*:Δ-sigH mutant was used to infect mice, bacterial burden comparable to *Mtb* was observed in lungs, in the absence of typical pathology [8]. These results in the NHP model are different. In response to *Mtb*, NHPs generate highly organized, humanlike granulomatous lesions, unlike mice [46]. It is thus conceivable that anti-*Mtb* responses (eg, hypoxia, oxidative stress) are more effective at the cellular level in the lungs of NHPs and are able to exert a greater degree of immune pressure on the bacilli. This could potentially explain why a mutant may be completely attenuated in the NHP model but only partially attenuated in the mouse model. In an unrelated study of the survival of hundreds of *Mtb* transposon mutants in NHP lungs, one-third of the mutants failed to survive in the NHP model [23]. In contrast, only 6%–10% of these mutants failed to survive in mice. Moreover, differences in primate vs murine immune system may account for the differential phenotypes of the SigH mutant in these species. In particular, our observations may directly result from the fact that reactive oxygen species play a greater role in primate immune system relative to the murine immune system where nitric oxide is more important. The importance of nitric oxide in primate tuberculosis is a matter of controversy reviewed by Tufariello et al [47]. It is possible that the loss of SigH regulon renders the mutant more susceptible to oxidants rather than to nitric oxide. We are now studying the early features of the immune response generated during early infection with the mutant and comparing it to the response generated by *Mtb*. Because the *Mtb*:Δ-sigH mutant is completely attenuated in NHPs, if a more robust immune response is observed, then this mutant may emerge as a candidate antitubercular vaccine. Interestingly, vaccination with a mutant in the related protein sigE protects against challenge with *Mtb* [48].

Notes

Author contributions. D. K. and A. A. L. were responsible for the funding; S. M. and D. K. were responsible for the research design; S. M., N. A. G., K. J. S., X. A., C. J. R., S. K. S., C. S., and A. H. performed the research; L. A. D., K. E. R.-L., and J. L. B. were responsible for the veterinary medicine; P. J. D. and A. A. L were responsible for veterinary pathology; D. K., S. M., and M. J. K. performed the data analysis; D. K. wrote the study with input from S. M. and A. A. L.

Financial support. This work was supported by the NIH (RR020159, AI089323, HL106790, AI091457, RR026006, and RR000164); Louisiana Board of Regents; Tulane Research Enhancement Fund; Tulane Center for Infectious Diseases; and Howard Hughes Medical Center-K-RITH.

Potential conflicts of interest. All authors: No reported conflicts.

All authors have submitted the ICMJE Form for Disclosure of Potential Conflicts of Interest. Conflicts that the editors consider relevant to the content of the manuscript have been disclosed.

References

1. Raviglione MC. The new Stop TB strategy and the Global Plan to Stop TB, 2006–2015. Bull World Health Organ **2007**; 85:327.
2. Gandhi NR, Moll A, Sturm AW, et al. Extensively drug-resistant tuberculosis as a cause of death in patients co-infected with tuberculosis and HIV in a rural area of South Africa. Lancet **2006**; 368:1575–80.
3. Adegbola RA, Hill PC, Secka O, et al. Surveillance of drug-resistant *Mycobacterium tuberculosis* in The Gambia. Int J Tuberc Lung Dis **2003**; 7:390–3.
4. Corbett EL, Watt CJ, Walker N, et al. The growing burden of tuberculosis: global trends and interactions with the HIV epidemic. Arch Intern Med **2003**; 163:1009–21.
5. Fine PE. Variation in protection by BCG: implications of and for heterologous immunity. Lancet **1995**; 346:1339–45.
6. Missiakas D, Raina S. The extracytoplasmic function sigma factors: role and regulation. Mol Microbiol **1998**; 28:1059–66.
7. Gomez JE, Chen JM, Bishai WR. Sigma factors of *Mycobacterium tuberculosis*. Tuber Lung Dis **1997**; 78:175–83.
8. Kaushal D, Schroeder BG, Tyagi S, et al. Reduced immunopathology and mortality despite tissue persistence in a *Mycobacterium tuberculosis* mutant lacking alternative sigma factor, SigH. Proc Natl Acad Sci U S A **2002**; 99:8330–5.
9. Manganelli R, Voskuil MI, Schoolnik GK, Dubnau E, Gomez M, Smith I. Role of the extracytoplasmic-function sigma factor sigma (H) in *Mycobacterium tuberculosis* global gene expression. Mol Microbiol **2002**; 45:365–74.
10. Raman S, Song T, Puyang X, Bardarov S, Jacobs WR Jr, Husson RN. The alternative sigma factor SigH regulates major components of oxidative and heat stress responses in *Mycobacterium tuberculosis*. J Bacteriol **2001**; 183:6119–25.
11. Rohde KH, Abramovitch RB, Russell DG. *Mycobacterium tuberculosis* invasion of macrophages: linking bacterial gene expression to environmental cues. Cell Host Microbe **2007**; 15:352–64.
12. Graham JE, Clark-Curtiss JE. Identification of *Mycobacterium tuberculosis* RNAs synthesized in response to phagocytosis by human macrophages by selective capture of transcribed sequences (SCOTS). Proc Natl Acad Sci U S A **1999**; 28:11554–9.
13. Mehra S, Dutta NK, Mollenkopf HJ, Kaushal D. *Mycobacterium tuberculosis* MT2816 encodes a key stress-response regulator. J Infect Dis **2010**; 202:943–53.
14. Ohno H, Zhu G, Mohan VP, et al. The effects of reactive nitrogen intermediates on gene expression in *Mycobacterium tuberculosis*. Cell Microbiol **2003**; 5:637–48.
15. Mehra S, Kaushal D. Functional genomics reveals extended roles of the *Mycobacterium tuberculosis* stress response factor sigmaH. J Bacteriol **2009**; 191:3965–80.
16. Fontán PA, Voskuil MI, Gomez M, et al. The *Mycobacterium tuberculosis* sigma factor sigmaB is required for full response to cell

envelope stress and hypoxia in vitro, but it is dispensable for in vivo growth. J Bacteriol **2009**; 191:5628–33.
17. Provvedi R, Boldrin F, Falciani F, Palù G, Manganelli R. Global transcriptional response to vancomycin in *Mycobacterium tuberculosis*. Microbiol **2009**; 155:1093–102.
18. Dutta NK, Mehra S, Kaushal D. A *Mycobacterium tuberculosis* sigma factor network responds to cell-envelope damage by the promising antimycobacterial thioridazine. PLoS One **2010**; 8:e10069.
19. Sherrid AM, Rustad TR, Cangelosi GA, Sherman DR. Characterization of a Clp protease gene regulator and the reaeration response in *Mycobacterium tuberculosis*. PLoS One **2010**; 6:e11622.
20. Dutta NK, Mehra S, Martinez AN, et al. The stress-response factor SigH modulates the interaction between *Mycobacterium tuberculosis* and host phagocytes. PLoS One. **2012;** 7: e28958.
21. Walsh GP, Tan EV, de la Cruz EC, et al. The Philippine cynomolgus monkey (*Macaca fasicularis*) provides a new nonhuman primate model of tuberculosis that resembles human disease. Nat Med **1996**; 2:430–6.
22. Capuano SV 3rd, Croix DA, Pawar S, et al. Experimental *Mycobacterium tuberculosis* infection of cynomolgus macaques closely resembles the various manifestations of human *M. tuberculosis* infection. Infect Immun **2003**; 71:5831–44.
23. Dutta NK, Mehra S, Didier PJ, et al. Genetic requirements for the survival of tubercle bacilli in primates. J Infect Dis **2010**; 201:1743–52.
24. Mehra S, Pahar B, Dutta NK, et al. Transcriptional reprogramming in nonhuman primate (rhesus macaque) tuberculosis granulomas. PLoS One **2010**; 5:e12266.
25. Mehra S, Golden NA, Dutta NK, et al. Reactivation of latent tuberculosis in rhesus macaques by co-infection with simian immunodeficiency virus. J Med Primatol **2011**; 40:233–43.
26. Gormus BJ, Blanchard JL, Alvarez XH, Didier PJ. Evidence for a rhesus monkey model of asymptomatic tuberculosis. J Med Primatol **2004**; 33:134–45.
27. Mansfield KG, Veazey RS, Hancock A, et al. Induction of disseminated *Mycobacterium avium* in simian AIDS is dependent upon simian immunodeficiency virus strain and defective granuloma formation. Am J Pathol **2001**; 159:693–702.
28. Hasegawa A, Liu H, Ling B, et al. The level of monocyte turnover predicts disease progression in the macaque model of AIDS. Blood **2009**; 114:2917–25.
29. Fontán PA, Aris V, Alvarez ME, et al. *Mycobacterium tuberculosis* sigma factor E regulon modulates the host inflammatory response. J Infect Dis **2008**; 198:877–85.
30. Saukkonen JJ, Bazydlo B, Thomas M, Strieter RM, Keane J, Kornfeld H. Beta-chemokines are induced by *Mycobacterium tuberculosis* and inhibit its growth. Infect Immun **2002**; 70:1684–93.
31. Velmurugan K, Chen B, Miller JL, et al. *Mycobacterium tuberculosis* nuoG is a virulence gene that inhibits apoptosis of infected host cells. PLoS Pathog **2007**; 3:e110.
32. Sadagopal S, Braunstein M, Hager CC, et al. Reducing the activity and secretion of microbial antitoxidants enhances the immunogenicity of BCG. PLoS One **2009**; 4:e5531.
33. Hinchey J, Lee S, Jeon BY, et al. Enhanced priming of adaptive immunity by a proapoptotic mutant of *Mycobacterium tuberculosis*. J Clin Invest **2007**; 117:2279–88.
34. Gill WP, Harik NS, Whiddon MR, Liao RP, Mittler JE, Sherman DR. A replication clock for *Mycobacterium tuberculosis*. Nat Med **2009**; 15:211–14.
35. Taylor JL, Hattle JM, Dreitz SA, et al. Role for matrix metalloproteinase 9 in granuloma formation during pulmonary *Mycobacterium tuberculosis* infection. Infect Immun **2006**; 74: 6135–44.
36. Volkman HE, Pozos TC, Zheng J, Davis JM, Rawls JF, Ramakrishnan L. Tuberculous granuloma induction via interaction of a bacterial secreted protein with host epithelium. Science **2010**; 327:466–9.
37. Allie N, Keeton R, Court N, et al. Limited role for lymphotoxin α in the host immune response to *Mycobacterium tuberculosis*. J Immunol **2010**; 185:4292–301.
38. Kumawat K, Pathak SK, Spetz AL, Kundu M, Basu J. Exogenous Nef is an inhibitor of *Mycobacterium tuberculosis*–induced tumor necrosis factor-a production and macrophage apoptosis. J Biol Chem **2010**; 285:12629–37.
39. Heibein JA, Goping IS, Barry M, et al. Granzyme B-mediated cytochrome c release is regulated by the Bcl-2 family members bid and Bax. J Exp Med **2000**; 192:1391–402.
40. Kernodle DS. Decrease in the effectiveness of bacille Calmette-Guerin vaccine against pulmonary tuberculosis: a consequence of increased immune suppression by microbial antioxidants, not over-attenuation. Clin Infect Dis **2010**; 15:177–84.
41. Romani L, Fallarino F, De Luca A, et al. Defective tryptophan catabolism underlies inflammation in mouse chronic granulomatous disease. Nature **2008**; 451:211–15.
42. Jo D, Liu D, Yao S, Collins RD, Hawiger J. Intracellular protein therapy with SOCS3 inhibits inflammation and apoptosis. Nat Med **2005**; 11:892–8.
43. Lin L, Spoor MS, Gerth AJ, Brody SL, Peng SL. Modulation of Th1 activation and inflammation by the NF-kappaB repressor Foxj1. Science **2004**; 303:1017–20.
44. Green AM, Mattila JT, Bigbee CL, Bongers KS, Lin PL, Flynn JL. $CD4^+$ regulatory T cells in a cynomolgus macaque model of *Mycobacterium tuberculosis* infection. J Infect Dis **2010**; 202:533–41.
45. Manrique SZ, Correa MA, Hoelzinger DB, et al. Foxp3-positive macrophages display immunosuppressive properties and promote tumor growth. J Exp Med **2011**; 208:1485–99.
46. Flynn JL. Lessons from experimental *Mycobacterium tuberculosis* infections. Microbes Infect **2006**; 8:1179–88.
47. Tufariello JM, Chan J, Flynn JL. Latent tuberculosis: mechanisms of host and bacillus that contribute to persistent infection. Lancet Infect Dis **2003**; 3:578–90.
48. Hernandez Pando R, Aguilar LD, Smith I, Manganelli R. Immunogenicity and protection induced by a *Mycobacterium tuberculosis* sigE mutant in a BALB/c mouse model of progressive pulmonary tuberculosis. Infect Immun **2010**; 78:3168–76.